

## Ionic conductivity enhancement in $\text{LiGe}_2(\text{PO}_4)_3$ solid electrolyte

Hiroshi Yamamoto<sup>a,\*</sup>, Mitsuharu Tabuchi<sup>b,1</sup>, Tomonari Takeuchi<sup>b,2</sup>, Hiroyuki Kageyama<sup>b,3</sup>,  
Osamu Nakamura<sup>b,4</sup>

<sup>a</sup> Advanced Technology Research Laboratories, Sumitomo Metal Industries, Ltd., 1 Nishino-cho Higashimukojima, Amagasaki, Hyogo 660, Japan

<sup>b</sup> Osaka National Research Institute, Agency of Industrial Science and Technology, MITI, 1-8-31 Midorigaoka, Ikeda, Osaka 563, Japan

Accepted 2 December 1996

### Abstract

In order to improve the ionic conductivity of  $\text{LiGe}_2(\text{PO}_4)_3$  as a solid electrolyte for lithium batteries, we have examined the effects of  $\text{Al}^{3+}$  and  $\text{Y}^{3+}$  substitution for  $\text{Ge}^{4+}$  and of  $\text{LiOH} \cdot \text{H}_2\text{O}$  addition on the ionic conductivity. The ionic conductivity of  $\text{LiGe}_2(\text{PO}_4)_3$  is enhanced four orders of magnitude by  $\text{Al}^{3+}$  addition, i.e.  $1.3 \times 10^{-4} \text{ S cm}^{-1}$  at 23 °C in case of the  $\text{Li}_{1-x}\text{Al}_x\text{Ge}_{2-x}(\text{PO}_4)_3$ . The addition of  $\text{Y}_2\text{O}_3$  or lithium salt also enhances the ionic conductivity because of the acceleration of the sintering process by the second phase of  $\text{Li}_4\text{P}_2\text{O}_7$ . © 1997 Elsevier Science S.A.

**Keywords:** Lithium germanium phosphate, Inorganic solid electrolytes, Ionic conductivity enhancement

### 1. Introduction

Lithium-ion conducting inorganic solid electrolytes have attracted much attention in application to all-solid rechargeable lithium batteries because of its thermal resistance and mechanical strength as separators. However, the ionic conductivity level of the solid electrolytes has not been as usual in practice, compared with conventional liquid electrolytes.

High  $\text{Li}^+$ -ion conductivity ( $\sim 10^{-3} \text{ S cm}^{-1}$  at room temperature) has recently been reported in the solid solution of  $\text{LiTi}_2(\text{PO}_4)_3$  [1,2] with the NASICON-type structure. In this compound, however, the multivalent nature of the titanium may induce an electronic conduction by the reduction of titanium(IV) to titanium(III) due to the presence of lithium metal in secondary batteries [3]. It is expected that the stable valence state (IV) of germanium in  $\text{LiGe}_2(\text{PO}_4)_3$  gives higher stability than titanium as an electronic insulator, although there have still been the problem of its low  $\text{Li}^+$ -ion conductivity [4].

Two possible ways to enhance the conductivity in  $\text{LiGe}_2(\text{PO}_4)_3$  have been proposed by Aono et al. [5,6]. One is substituting  $\text{M}^{3+}$  for  $\text{Ge}^{4+}$  and the other is making a com-

posite with some lithium salts. They observed a conductivity enhancement in both cases, although the enhancing mechanisms in the latter case have not yet been fully understood.

In the present study, therefore, we have tried to improve the ionic conductivity of  $\text{LiGe}_2(\text{PO}_4)_3$  by addition of either  $\text{M}_2\text{O}_3$  ( $\text{M} = \text{Al}$  and  $\text{Y}$ ) or lithium salt. The difference in the main factor controlling the conductivity enhancement between the two systems will be also discussed.

### 2. Experimental

$\text{Li}_{1+x}\text{M}_x\text{Ge}_{2-x}(\text{PO}_4)_3$  specimens ( $\text{M} = \text{Al}$  and  $\text{Y}$ ) were prepared by solid-state reaction from stoichiometric mixtures of  $\text{LiOH} \cdot \text{H}_2\text{O}$ ,  $\text{NH}_4\text{H}_2\text{PO}_4$ ,  $\text{GeO}_2$ , and  $\text{M}_2\text{O}_3$ . In addition, in order to examine the effect of the second phase,  $\text{LiGe}_2(\text{PO}_4)_3$ /lithium salt composites were prepared by adding extra  $\text{LiOH} \cdot \text{H}_2\text{O}$ , as compared with the stoichiometry of  $\text{LiGe}_2(\text{PO}_4)_3$ . After reacting at 900 °C for 2 h in air, these compounds were grounded in a ball mill for 12 h. This procedure was repeated in the same manner to complete the solid-state reaction. Then the reacted powder was pressed into pellets and sintered at 900 °C for 2 h.  $\text{GeO}_2$  and  $\text{Li}_4\text{P}_2\text{O}_7$  were recognized by X-ray diffraction (XRD) analysis in the above-described  $\text{Li}_{1+x}\text{Al}_x\text{Ge}_{2-x}(\text{PO}_4)_3$  specimen when  $x$  was greater than 0.4,  $\text{Li}_{1+x}\text{Y}_x\text{Ge}_{2-x}(\text{PO}_4)_3$  specimens, and  $\text{LiGe}_2(\text{PO}_4)_3$ /lithium salt composites. In order to examine the effect of each second phase individually, composite mate-

\* Corresponding author. Tel. +81 (6) 411 7745, Fax: +81 (6) 411 7796.

<sup>1</sup> Tel.: +81 (727) 51 9618; Fax: +81 (727) 51 9714

<sup>2</sup> Tel.: +81 (727) 51 9618; Fax: +81 (727) 51 9714.

<sup>3</sup> Tel.: +81 (727) 51 9618; Fax: +81 (727) 51 9714

<sup>4</sup> Tel.: +81 (727) 51 9618; Fax: +81 (727) 51 9714.

rials of  $\text{LiGe}_2(\text{PO}_4)_3/\text{GeO}_2$  and  $\text{LiGe}_2(\text{PO}_4)_3/\text{Li}_4\text{P}_2\text{O}_7$  were prepared by using the  $\text{LiGe}_2(\text{PO}_4)_3$  obtained in the above procedure. Here the  $\text{Li}_4\text{P}_2\text{O}_7$  was synthesized by a solid-state reaction, as we could not obtain the commercially available powder.

After sintering, powder specimens obtained by crushing the pellets were characterized by XRD analysis performed on a Rigaku RINT1500 using  $\text{Cu K}\alpha$  radiation. The lattice constants of  $\text{Li}_{1+x}\text{M}_x\text{Ge}_{2-x}(\text{PO}_4)_3$  indexed to the hexagonal unit cell were determined by means of a least-square refinement of the  $d$ -spacing values calibrated by using high purity Si powder as an internal standard. Further, the powder specimens were characterized by differential thermal analysis (DTA) performed on Rigaku TAS-200 in air at a heating and a cooling rate of  $10^\circ\text{C}/\text{min}$ . The bulk density of the sintered pellets was calculated by measuring their weight and volume. The ionic conductivity data of the sintered pellets were obtained by complex impedance measurements using a frequency response analyzer (NF Electric Instrument 5020) and potentiostat (Hokuto Denko HA501) in the frequency range from 0.1 Hz to 20 kHz in an argon atmosphere. The blocking gold electrodes were formed on both sides of the pellets from Engelhard A-3360 paste by heating to  $600^\circ\text{C}$  over a period of 20 min.

### 3. Results and discussion

XRD patterns of the nominal  $\text{Li}_{1+x}\text{Al}_x\text{Ge}_{2-x}(\text{PO}_4)_3$  specimens were shown in Fig. 1. It was confirmed that the obtained stoichiometric  $\text{LiGe}_2(\text{PO}_4)_3$  has rhombohedral structure ( $R\bar{3}c$ ) without any other phases. When  $x$  was not greater than 0.4, only a single rhombohedral phase was detected. In the case of a great Al content ( $x=0.6$ ), extra second phases such as  $\text{GeO}_2$  and  $\text{Li}_4\text{P}_2\text{O}_7$  were observed. The lattice volume increased significantly with increasing Al content, as summarized in Table 1. The lattice volume value and its tendency to Al content are consistent with the results reported by Aono et al. [5]. The above XRD results indicate

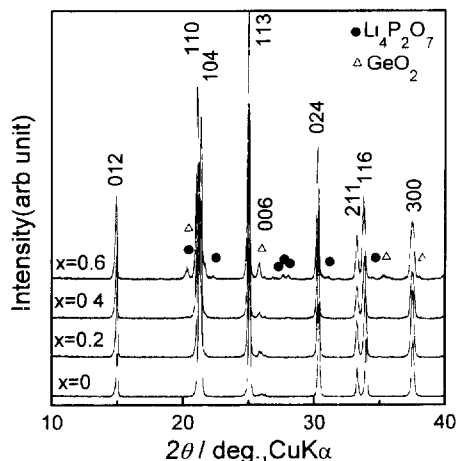


Fig. 1 XRD patterns of the  $\text{Li}_{1+x}\text{Al}_x\text{Ge}_{2-x}(\text{PO}_4)_3$  system where  $x = 0, 0.2, 0.4, 0.6$ .

that  $\text{Al}^{3+}$  can be incorporated into the  $\text{LiGe}_2(\text{PO}_4)_3$  lattice until  $x=0.4$ . The  $\text{Ge}^{4+}$  in  $\text{LiGe}_2(\text{PO}_4)_3$  will probably be replaced by  $\text{Al}^{3+}$  because the ionic radius of  $\text{Al}^{3+}$  ( $0.53 \text{ \AA}$ ) is close to that of the  $\text{Ge}^{4+}$  ( $0.54 \text{ \AA}$ ). If the simple substitution of  $\text{Al}^{3+}$  for  $\text{Ge}^{4+}$  occurred, the lattice volume will be almost constant with increasing the Al content. However, the experimental data could not be explained by this simple substitution model. Therefore, additional  $\text{Li}^+$  inserted to the  $\text{LiGe}_2(\text{PO}_4)_3$  lattice for keeping the charge neutrality can be responsible for the small increase in lattice volume. In this point, it is necessary to perform a precise structural study for the series of the  $\text{Li}_{1+x}\text{Al}_x\text{Ge}_{2-x}(\text{PO}_4)_3$  specimens.

In the case of the nominal  $\text{Li}_{1+x}\text{Y}_x\text{Ge}_{2-x}(\text{PO}_4)_3$  specimens, the product was actually a mixture of rhombohedral phase ( $\text{LiGe}_2(\text{PO}_4)_3$ -based solid solution),  $\text{YPO}_4$ ,  $\text{GeO}_2$ , and  $\text{Li}_4\text{P}_2\text{O}_7$  even at  $x=0.2$ , as can be seen from the comparison between the curves (a) and (e), (f) in Fig. 2. Although the  $a$ - and  $c$ -axis parameters and the lattice volume of the rhombohedral phase were close to those of the original  $\text{LiGe}_2(\text{PO}_4)_3$  (see Table 1), these values changed monotonously with the Y content. These results imply that the rhombohedral phases are not regarded as the original

Table 1

Unit cell parameters of the  $\text{Li}_{1+x}\text{M}_x\text{Ge}_{2-x}(\text{PO}_4)_3$  ( $\text{M} = \text{Al}$  and  $\text{Y}$ ) system and  $\text{LiGe}_2(\text{PO}_4)_3$ /lithium salt composite indexed in a hexagonal unit cell

Sample		$a$ ( $\text{\AA}$ )	$c$ ( $\text{\AA}$ )	$V$ ( $\text{\AA}^3$ )
$\text{LiGe}_2(\text{PO}_4)_3$		8.2829(2)	20.501(1)	1218.1(1)
$\text{Li}_{1+x}\text{Al}_x\text{Ge}_{2-x}(\text{PO}_4)_3$	$x=0.2$	8.2894(8)	20.541(4)	1222.3(2)
	$x=0.4$	8.2771(7)	20.629(4)	1223.9(2)
$\text{Li}_{1+x}\text{Y}_x\text{Ge}_{2-x}(\text{PO}_4)_3$	$x=0.2^a$	8.2803(7)	20.528(4)	1218.9(2)
	$x=0.4^a$	8.2793(10)	20.548(5)	1219.8(3)
$\text{LiGe}_2(\text{PO}_4)_3$ /lithium salt composite	16% <sup>b</sup>	8.2811(10)	20.526(5)	1219.0(3)
	33% <sup>b</sup>	8.2827(9)	20.516(5)	1218.9(3)

<sup>a</sup> Nominal composition.

<sup>b</sup> The % shows the amount of extra  $\text{LiOH}\cdot\text{H}_2\text{O}$  added to the starting materials, as compared with the stoichiometry of  $\text{LiGe}_2(\text{PO}_4)_3$ .

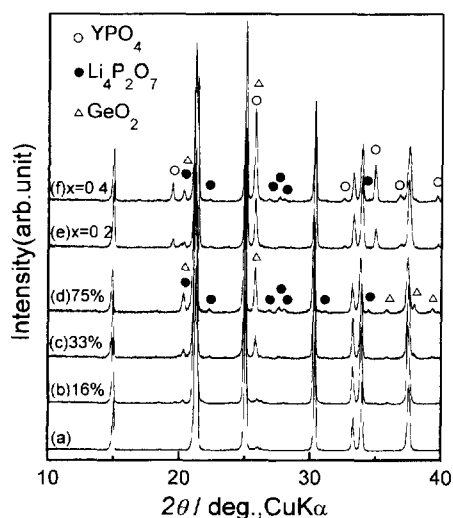


Fig. 2. XRD patterns of (a)  $\text{LiGe}_2(\text{PO}_4)_3$ , (b)–(d)  $\text{LiGe}_2(\text{PO}_4)_3$ /lithium salt composite, and (e)–(f) nominal  $\text{Li}_{1+x}\text{Y}_x\text{Ge}_{2-x}(\text{PO}_4)_3$  system. The % shows the amount of extra  $\text{LiOH}\cdot\text{H}_2\text{O}$  added to the starting materials, as compared with the stoichiometry of  $\text{LiGe}_2(\text{PO}_4)_3$ .

$\text{LiGe}_2(\text{PO}_4)_3$ . However, the formation of  $\text{YPO}_4$  and large difference in ionic radius between  $\text{Ge}^{4+}$  (0.54 Å) and  $\text{Y}^{3+}$  (0.89 Å) exclude the simple  $\text{Y}^{3+}$  substitution model for the  $\text{Ge}^{4+}$  in  $\text{LiGe}_2(\text{PO}_4)_3$ . The clarification of the effect of extra lithium on the lattice of  $\text{LiGe}_2(\text{PO}_4)_3$  was needed for the understanding of the structure of the rhombohedral phase. Therefore, we checked the products of  $\text{LiGe}_2(\text{PO}_4)_3$ /lithium salt composites as shown in Fig. 2(b)–(d). Each  $\text{LiGe}_2(\text{PO}_4)_3$ /lithium salt composite was the mixture of a rhombohedral phase ( $\text{LiGe}_2(\text{PO}_4)_3$ -based solid solution),  $\text{GeO}_2$ , and  $\text{Li}_4\text{P}_2\text{O}_7$ , similar to the case of the nominal  $\text{Li}_{1+x}\text{Y}_x\text{Ge}_{2-x}(\text{PO}_4)_3$  specimens except for  $\text{YPO}_4$  formation. The shift of each XRD peak for the rhombohedral phase was quite small with increasing the amount of initial lithium salt. Both the  $a$ - and  $c$ -axis parameters and the lattice volume of the rhombohedral phase were close to those of the rhombohedral one in the nominal  $\text{Li}_{1+x}\text{Y}_x\text{Ge}_{2-x}(\text{PO}_4)_3$  system, indicating that a rhombohedral phase presented in  $\text{LiGe}_2(\text{PO}_4)_3$ /lithium salt composites can be regarded as that obtained from the  $\text{Li}_{1+x}\text{Y}_x\text{Ge}_{2-x}(\text{PO}_4)_3$  system. Using the three series of specimens, we measured the electrical conductivity by the a.c. impedance method.

The results of conductivity and density measurement were shown in Fig. 3 for the nominal  $\text{Li}_{1+x}\text{M}_x\text{Ge}_{2-x}(\text{PO}_4)_3$  ( $\text{M} = \text{Al}$  and  $\text{Y}$ ) systems and Fig. 4 for  $\text{LiGe}_2(\text{PO}_4)_3$ /lithium salt composites. The complex impedance plots for each specimen produced only a single semicircle between 0.1 Hz and 20 kHz, which was insufficient to separate it into two semicircles, i.e. a bulk and a grain boundary components. Therefore, we treated the conductivity data as a total one containing both the bulk and the grain boundary conduction. By  $\text{Al}^{3+}$  incorporation, the conductivity of  $\text{LiGe}_2(\text{PO}_4)_3$  was greatly enhanced and its apparent activation energy of  $\text{Li}^+$ -ion migration estimated from the Arrhenius plots of the total conductivity was lowered with increasing Al content up to

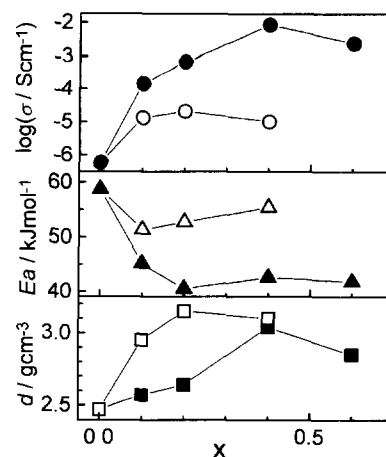


Fig. 3. Conductivity at 127 °C, activation energy, and bulk density of (●,▲,■) the  $\text{Li}_{1+x}\text{Al}_x\text{Ge}_{2-x}(\text{PO}_4)_3$  system and (○,□) the nominal  $\text{Li}_{1+x}\text{Y}_x\text{Ge}_{2-x}(\text{PO}_4)_3$  system. The ionic conductivity data of the  $\text{Li}_{1+x}\text{Al}_x\text{Ge}_{2-x}(\text{PO}_4)_3$  system where  $x = 0.2, 0.4, 0.6$  is estimated by extrapolation of the linear  $\log \sigma T$  vs.  $T^{-1}$  plot from the data at lower temperatures.

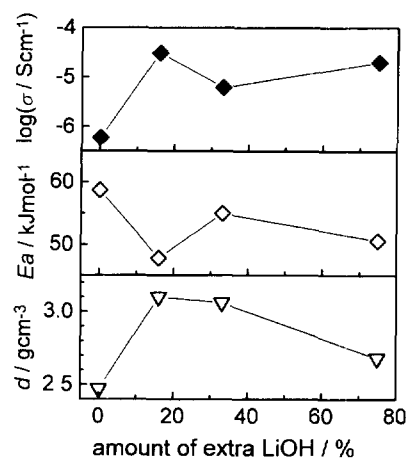


Fig. 4. Conductivity at 127 °C, activation energy, and bulk density of  $\text{LiGe}_2(\text{PO}_4)_3$ /lithium salt composites as a function of the amount of extra  $\text{LiOH}\cdot\text{H}_2\text{O}$  added to the starting materials, as compared with the stoichiometry of  $\text{LiGe}_2(\text{PO}_4)_3$ .

0.4 per chemical formula. Lowering the conductivity above 0.4 of Al content could be attributed to the formation of the second phases such as  $\text{GeO}_2$  and  $\text{Li}_4\text{P}_2\text{O}_7$ . The conductivity enhancement will probably be attributed to the increase in mobility and concentration of mobile  $\text{Li}^+$  ions with increasing Al content up to 0.4. The change in mobility of mobile  $\text{Li}^+$  ions may relate to the change in lattice volume. The maximum conductivity achieved was  $1.3 \times 10^{-4} \text{ S cm}^{-1}$  for  $x = 0.4$  even at 23 °C. We can propose that the  $\text{Li}_{1+x}\text{Al}_x\text{Ge}_{2-x}(\text{PO}_4)_3$  specimens would be a promising inorganic solid electrolytes for all-solid lithium batteries.

On the other hand, the conductivity of both the nominal  $\text{Li}_{1+x}\text{Y}_x\text{Ge}_{2-x}(\text{PO}_4)_3$  specimens and the  $\text{LiGe}_2(\text{PO}_4)_3$ /lithium salt composites was one and a half orders of magnitude higher and the apparent activation energy of both of them was lower than those of  $\text{LiGe}_2(\text{PO}_4)_3$ , despite the presence of impurities. Therefore, the effect of the second phase on the conductivity was needed for understanding the enhancement

of both the nominal  $\text{Li}_{1+x}\text{Y}_t\text{Ge}_{2-x}(\text{PO}_4)_3$  specimens and the  $\text{LiGe}_2(\text{PO}_4)_3$ /lithium salt composites.

Fig. 5 shows the Arrhenius plots of the conductivity for  $\text{LiGe}_2(\text{PO}_4)_3$ ,  $\text{LiGe}_2(\text{PO}_4)_3$  sintered with either 10 mol%  $\text{GeO}_2$  or  $\text{Li}_4\text{P}_2\text{O}_7$ , and  $\text{Li}_4\text{P}_2\text{O}_7$  only. The sintering temperature of above four specimens was 900 °C. Both the  $\text{LiGe}_2(\text{PO}_4)_3$  containing  $\text{GeO}_2$  and the  $\text{Li}_4\text{P}_2\text{O}_7$  itself exhibited poor conductivity compared with that of original  $\text{LiGe}_2(\text{PO}_4)_3$ , indicating that both  $\text{GeO}_2$  and  $\text{Li}_4\text{P}_2\text{O}_7$  act as insulators for  $\text{Li}^+$ -ion conduction. However,  $\text{LiGe}_2(\text{PO}_4)_3$  containing a small amount of  $\text{Li}_4\text{P}_2\text{O}_7$  had a higher conductivity than that of the  $\text{LiGe}_2(\text{PO}_4)_3$ . This situation is quite similar with those of the nominal  $\text{Li}_{1+x}\text{Y}_t\text{Ge}_{2-x}(\text{PO}_4)_3$  specimens and the  $\text{LiGe}_2(\text{PO}_4)_3$ /lithium salt composites (see Figs. 3 and 4). We noticed that some 'composite effect' of  $\text{LiGe}_2(\text{PO}_4)_3/\text{Li}_4\text{P}_2\text{O}_7$  may play an important role in the conductivity enhancement of above two types of the specimen. The sintering temperature dependence of the conductivity and density of  $\text{LiGe}_2(\text{PO}_4)_3$  containing  $\text{Li}_4\text{P}_2\text{O}_7$  were shown in Fig. 6. Both the conductivity and the density increased with increasing sintering temperature. Especially a great difference in these data were observed between 600 and 700 °C, that is, the relatively dense pellet with high conductivity compared with those of  $\text{LiGe}_2(\text{PO}_4)_3$  could be obtained by sintering above 700 °C. In order to examine the thermal behavior of the specimens, DTA measurements were performed on heating as shown in Fig. 7. No thermal anomaly was detected for both  $\text{LiGe}_2(\text{PO}_4)_3$  and  $\text{Li}_{1.2}\text{Al}_{0.2}\text{Ge}_{1.8}(\text{PO}_4)_3$ . On the other hand, three endothermic peaks were observed at 583, 646, and 882 °C (peak top position) on heating. These three peaks were also detected as exothermic ones on cooling at 506, 636, and 835 °C, which are the indication of the reversible phase transitions. Concerning the thermal behavior of  $\text{Li}_4\text{P}_2\text{O}_7$ , Tien and Hummel [7] reported that  $\text{Li}_4\text{P}_2\text{O}_7$  exhibits a structural change at 630 °C and melts at 885 °C. However, we have no information on the lowest phase transition point. DTA curves of  $\text{LiGe}_2(\text{PO}_4)_3$  and  $\text{Li}_4\text{P}_2\text{O}_7$  mixture, nominal  $\text{Li}_{1.2}\text{Y}_{0.2}\text{Ge}_{1.8}(\text{PO}_4)_3$ , and  $\text{LiGe}_2(\text{PO}_4)_3$ /lithium salt composite revealed at least two endothermic peaks which were situated at about 650 and 730–

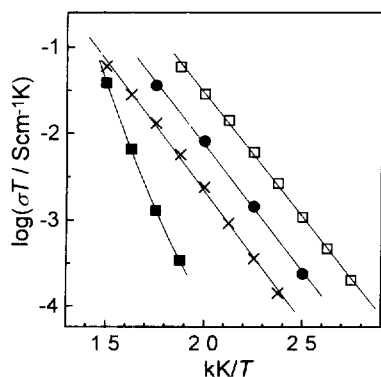


Fig. 5 Arrhenius plots of conductivity for (●)  $\text{LiGe}_2(\text{PO}_4)_3$ ,  $\text{LiGe}_2(\text{PO}_4)_3$  sintered with either (+) 10 mol%  $\text{GeO}_2$  or (□)  $\text{Li}_4\text{P}_2\text{O}_7$ , and (■)  $\text{Li}_4\text{P}_2\text{O}_7$  only.

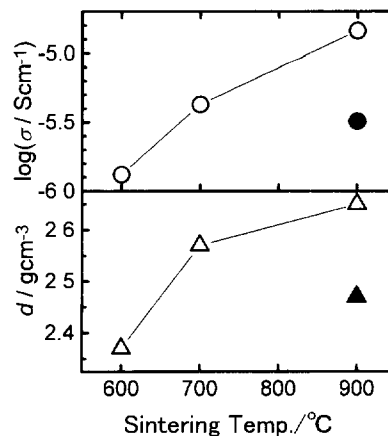


Fig. 6 Sintering temperature dependence of conductivity at 171 °C and bulk density of (○, ●)  $\text{LiGe}_2(\text{PO}_4)_3$  sintered with 20 mol%  $\text{Li}_4\text{P}_2\text{O}_7$  and (△, ▲)  $\text{LiGe}_2(\text{PO}_4)_3$  only.

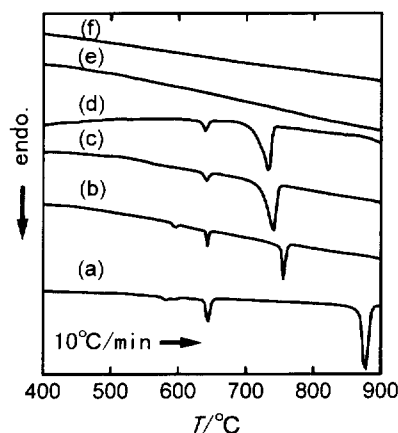


Fig. 7. DTA curves of (a)  $\text{Li}_4\text{P}_2\text{O}_7$ , (b) mixture of  $\text{LiGe}_2(\text{PO}_4)_3$  and  $\text{Li}_4\text{P}_2\text{O}_7$ , (c)  $\text{LiGe}_2(\text{PO}_4)_3$ /lithium salt composite (extra 33 mol%  $\text{LiOH}\cdot\text{H}_2\text{O}$  was added to the starting materials, as compared with the stoichiometry of  $\text{LiGe}_2(\text{PO}_4)_3$ ), (d) nominal  $\text{Li}_{1.2}\text{Y}_{0.2}\text{Ge}_{1.8}(\text{PO}_4)_3$ , (e)  $\text{Li}_{1.2}\text{Al}_{0.2}\text{Ge}_{1.8}(\text{PO}_4)_3$ , and (f)  $\text{LiGe}_2(\text{PO}_4)_3$ .

750 °C on heating. Since the former transition temperature could be attributed to the structural changing temperature of  $\text{Li}_4\text{P}_2\text{O}_7$ , the latter one could be attributed to the melting temperature of  $\text{Li}_4\text{P}_2\text{O}_7$ -based eutectic mixture. The melting point at about 740 °C for nominal  $\text{Li}_{1.2}\text{Y}_{0.2}\text{Ge}_{1.8}(\text{PO}_4)_3$ , and  $\text{LiGe}_2(\text{PO}_4)_3$ /lithium salt composite are very close to the changing point in both the density and the conductivity of  $\text{LiGe}_2(\text{PO}_4)_3/\text{Li}_4\text{P}_2\text{O}_7$  composite (see Fig. 6). Further, Figs. 3 and 4 show that the densification of the sintered pellets leads to high conductivity because the dense  $\text{LiGe}_2(\text{PO}_4)_3$  pellet was hardly obtained by sintering only  $\text{LiGe}_2(\text{PO}_4)_3$  powder at 900 °C. Therefore, we can conclude that the conductivity enhancement in both the nominal  $\text{Li}_{1+x}\text{Y}_t\text{Ge}_{2-x}(\text{PO}_4)_3$  specimens and  $\text{LiGe}_2(\text{PO}_4)_3$ /lithium salt composites has been attributed mainly to the densification of the pellets by lowering the melting point for  $\text{Li}_4\text{P}_2\text{O}_7$ -based eutectic mixture.

#### 4. Conclusions

The ionic conductivity of poorly conductive  $\text{LiGe}_2(\text{PO}_4)_3$  was enhanced four orders of magnitude by incorporating  $\text{Al}^{3+}$  into the  $\text{LiGe}_2(\text{PO}_4)_3$  lattice. The ionic conductivity was also enhanced one and a half orders of magnitude by adding  $\text{Y}_2\text{O}_3$  or lithium salt such as  $\text{LiOH}\cdot\text{H}_2\text{O}$ . The conductivity enhancement in the latter case may be responsible for the increase in sinterability due to the lowering of the melting point for  $\text{Li}_4\text{P}_2\text{O}_7$  by formation of eutectic mixture mainly with  $\text{LiGe}_2(\text{PO}_4)_3$ . Such  $\text{Al}^{3+}$ -doped  $\text{LiGe}_2(\text{PO}_4)_3$  and  $\text{LiGe}_2(\text{PO}_4)_3/\text{Li}_4\text{P}_2\text{O}_7$  composite would be promising materials as inorganic solid electrolytes for all-solid lithium batteries.

#### References

- [1] M.A. Subramanian, R. Subramanian and A. Clearfield, *Solid State Ionics*, 18/19 (1986) 562–569.
- [2] H. Aono, E. Sugimoto, Y. Sadaoka, N. Imanaka and G. Adachi, *J Electrochem. Soc.*, 136 (1989) 590–591
- [3] C. Delmas, A. Nadiri and J.L. Soubeyroux, *Solid State Ionics*, 28–30 (1988) 419–423.
- [4] S.-C. Li, J.-Y. Cai and Z.-X. Lin, *Solid State Ionics*, 28–30 (1988) 1265–1270.
- [5] H. Aono, E. Sugimoto, Y. Sadaoka, N. Imanaka and G. Adachi, *Bull. Chem. Soc. Jpn.*, 65 (1992) 2200–2204.
- [6] H. Aono, E. Sugimoto, Y. Sadaoka, N. Imanaka and G. Adachi, *J. Electrochem. Soc.*, 140 (1993) 1827–1833
- [7] T.Y. Tien and F.A. Hummel, *J. Am. Ceram. Soc.*, 44 (1961) 206–208.